Proteogenomic Characterization of Bladder Cancer Reveals Sensitivity to Apoptosis Induced by Tumor Necrosis Factor–related Apoptosis-inducing Ligand in FGFR3-mutated Tumors

Clarice Groeneveld, Virginia Sanchez-Quiles, Florent Dufour, Mingjun Shi, Florent Dingli, Rémy Nicolle, Elodie Chapeaublanc, Patrick Poullet, Daniel Jeffery, Clémentine Krucker, et al.

EUROPEAN UROLOGY xxx (xxxx) xxx–xxx

available at www.sciencedirect.com
journal homepage: www.europeanurology.com

European Association of Urology

Bladder Cancer

Proteogenomic Characterization of Bladder Cancer Reveals Sensitivity to Apoptosis Induced by Tumor Necrosis Factor–related Apoptosis-inducing Ligand in *FGFR3*-mutated Tumors

Clarice S. Groeneveld [a,b,†], *Virginia Sanchez-Quiles* [a,†], *Florent Dufour* [a,c,†], *Mingjun Shi* [a,d], *Florent Dingli* [e], *Rémy Nicolle* [f], *Elodie Chapeaublanc* [a], *Patrick Poullet* [g], *Daniel Jeffery* [h], *Clémentine Krucker* [a], *Pascale Maillé* [i], *Francis Vacherot* [j], *Dimitri Vordos* [k], *Simone Benhamou* [l], *Thierry Lebret* [m], *Olivier Micheau* [n], *Andrei Zinovyev* [g], *Damarys Loew* [e], *Yves Allory* [a,o,‡], *Aurélien de Reyniès* [b,‡], *Isabelle Bernard-Pierrot* [a,‡,*], *François Radvanyi* [a,‡,*]

[a] *Equipe labellisée Ligue Contre le Cancer, CNRS, UMR144, Institut Curie, PSL Research University, Paris, France;* [b] *Centre de Recherche des Cordeliers, AP-HP, Université Paris Cité, Paris, France;* [c] *Inovarion, Paris, France;* [d] *Department of Urology, Beijing Friendship Hospital, Capital Medical University, Beijing, China;* [e] *Centre de Recherche, CurieCoreTech Mass Spectrometry Proteomics, Institut Curie, PSL Research University, Paris, France;* [f] *Centre de Recherche sur l'Inflammation (CRI), INSERM, U1149, CNRS, ERL 8252, Université Paris Cité, Paris, France;* [g] *INSERM U900, MINES ParisTech, Institut Curie, PSL Research University, Paris, France;* [h] *Urology Medico-Scientific Program, Department of Translational Research, Institut Curie, PSL Research University, Paris, France;* [i] *Département de Pathologie, Hôpital Henri Mondor, APHP, Créteil, France;* [j] *Université Paris Est Créteil, TRePCa, Créteil, France;* [k] *Service d'Urologie, Hôpital Henri Mondor, APHP, Créteil, France;* [l] *Gustave Roussy, INSERM U1018, Villejuif, France;* [m] *Service d'Urologie, Hôpital Foch, UVSQ, Université Paris-Saclay, Suresnes, France;* [n] *INSERM, LNC UMR1231, Université Bourgogne Franche-Comté, Dijon, France;* [o] *Department of Pathology, Institut Curie, UVSQ, Université Paris-Saclay, Saint-Cloud, France*

Article info

Article history:
Accepted May 26, 2023

Associate Editor:
James Catto

Statistical Editor:
Andrew Vickers

Keywords:
Apoptosis
Bladder cancer
FGFR3

Abstract

Background: Molecular understanding of muscle-invasive (MIBC) and non–muscle-invasive (NMIBC) bladder cancer is currently based primarily on transcriptomic and genomic analyses.
Objective: To conduct proteogenomic analyses to gain insights into bladder cancer (BC) heterogeneity and identify underlying processes specific to tumor subgroups and therapeutic outcomes.
Design, setting, and participants: Proteomic data were obtained for 40 MIBC and 23 NMIBC cases for which transcriptomic and genomic data were already available. Four BC-derived cell lines harboring *FGFR3* alterations were tested with interventions.
Intervention: Recombinant tumor necrosis factor-related apoptosis-inducing ligand (TRAIL), second mitochondrial–derived activator of caspases mimetic (birinapant), pan-FGFR inhibitor (erdafitinib), and *FGFR3* knockdown.

† These authors contributed equally to the work.
‡ These authors co-supervised the work equally.
* Corresponding authors. Equipe labellisée Ligue Contre le Cancer, CNRS, UMR144, Institut Curie, PSL Research University, Paris, France. Tel. +33 156 246 357 (F. Radvanyi). Equipe labellisée Ligue Contre le Cancer, CNRS, UMR144, Institut Curie, PSL Research University, Paris, France (I. Bernard-Pierrot).
E-mail address: francois.radvanyi@curie.fr (F. Radvanyi).

https://doi.org/10.1016/j.eururo.2023.05.037

Please cite this article as: C.S. Groeneveld, V. Sanchez-Quiles, F. Dufour et al., Proteogenomic Characterization of Bladder Cancer Reveals Sensitivity to Apoptosis Induced by Tumor Necrosis Factor–related Apoptosis-inducing Ligand in *FGFR3*-mutated Tumors, Eur Urol (2023), https://doi.org/10.1016/j.eururo.2023.05.037

Proteogenomics
Proteomics
Tumor necrosis factor–related apoptosis-inducing ligand
Tumor necrosis factor–related apoptosis-inducing ligand receptors

Outcome measurements and statistical analysis: Proteomic groups from unsupervised analyses (uPGs) were characterized using clinicopathological, proteomic, genomic, transcriptomic, and pathway enrichment analyses. Additional enrichment analyses were performed for *FGFR3*-mutated tumors. Treatment effects on cell viability for *FGFR3*-altered cell lines were evaluated. Synergistic treatment effects were evaluated using the zero interaction potency model.

Results and limitations: Five uPGs, covering both NMIBC and MIBC, were identified and bore coarse-grained similarity to transcriptomic subtypes underlying common features of these different entities; uPG-E was associated with the Ta pathway and enriched in *FGFR3* mutations. Our analyses also highlighted enrichment of proteins involved in apoptosis in *FGFR3*-mutated tumors, not captured through transcriptomics. Genetic and pharmacological inhibition demonstrated that FGFR3 activation regulates TRAIL receptor expression and sensitizes cells to TRAIL-mediated apoptosis, further increased by combination with birinapant.

Conclusions: This proteogenomic study provides a comprehensive resource for investigating NMIBC and MIBC heterogeneity and highlights the potential of TRAIL-induced apoptosis as a treatment option for *FGFR3*-mutated bladder tumors, warranting a clinical investigation.

Patient summary: We integrated proteomics, genomics, and transcriptomics to refine molecular classification of bladder cancer, which, combined with clinical and pathological classification, should lead to more appropriate management of patients. Moreover, we identified new biological processes altered in *FGFR3*-mutated tumors and showed that inducing apoptosis represents a new potential therapeutic option.

1. Introduction

Bladder cancer presents either as non–muscle-invasive bladder cancer (NMIBC; 70–75% of patients) or as muscle-invasive bladder cancer (MIBC; 25–30% of patients). Among NMIBC cases, about 70% are noninvasive papillary urothelial carcinoma, low or high grade (stage pTa); 1–3% urothelial carcinoma in situ (CIS), a flat high-grade lesion (pTis); and the remainder invasive urothelial carcinoma (pT1), virtually all high grade [1]. From clinical, pathological, and molecular data, two major pathways have been proposed in bladder cancer [2,3]. The pTa low-grade papillary pathway has a low risk of progression to MIBC. The second pathway progresses along CIS and/or pTa high-grade papillary urothelial carcinoma to pT1 and muscle-invasive tumors. Activating point mutations of the tyrosine kinase receptor FGFR3 are a common molecular feature of pTa low-grade papillary tumors but are also encountered in 12–15% MIBC cases [4].

Five-year survival rates for NMIBC patients are favorable (>90%) [5], but MIBC is an aggressive disease associated with a 5-yr survival rate of 60% for patients with localized disease and <10% for patients with distant metastasis [6]. Despite the advent of immunotherapy and targeted therapies, ∼75% of patients treated with immune checkpoint therapy [7] and ∼55% of patients with *FGFR3* mutations treated with the anti-FGFR erdafitinib [8] exhibit no response, demonstrating the need for a deeper understanding of bladder cancer biology.

RNA- and DNA-based "omic" analyses of bladder cancer have revealed clear molecular heterogeneity and led to the identification of subtypes in both NMIBC and MIBC [4,9–15]. The most recent transcriptomic classification of NMIBC [15] identified four subtypes: classes 1 and 3, both enriched in *FGFR3*-mutated tumors; class 2a, an aggressive subtype; and class 2b, an immune-infiltrated subtype. Concerning MIBC, an international consensus transcriptomic classification identified six consensus subtypes (luminal papillary, luminal unstable, luminal nonspecified, basal/squamous (Ba/Sq), stroma rich, and neuroendocrine like) [16]. The luminal papillary subtype includes the majority of *FGFR3*-mutated MIBC tumors.

High-throughput proteomics through liquid chromatography coupled to tandem mass spectrometry (LC-MS/MS) is increasingly used to study cancer [17]. Integration of protein data with transcriptomics and genomics constitutes a new fast-growing field of cancer research, leading to a better understanding of the molecular basis of cancer and accelerating the translation of molecular findings into the clinic [17,18]. This approach has already been applied in several cancers [17–24] with the potential to improve therapeutic outcomes.

Stroggilos et al [25] were the first to apply high-throughput proteomics to a large bladder cancer cohort. Recently, Xu et al [26] integrated matched proteomic, transcriptomic, and genomic data from formalin-fixed paraffin-embedded tumors.

Here, we extend recent efforts to provide integrated proteogenomic characterization of bladder cancer by performing a joint proteome, transcriptome, and genome analysis of 63 fresh frozen samples (23 NMIBC and 40 MIBC).

2. Patients and methods

For detailed methods, see the Supplementary material.

2.1. Patients

Sixty-three bladder tumors were studied. Clinical and histopathological features [1] including age, gender, invasiveness, World Health Organization grade, tumor stage, histological subtypes, presence of CIS [27], and papillary and/or endophytic growth pattern are summarized in Supplementary Table 1.

Please cite this article as: C.S. Groeneveld, V. Sanchez-Quiles, F. Dufour et al., Proteogenomic Characterization of Bladder Cancer Reveals Sensitivity to Apoptosis Induced by Tumor Necrosis Factor–related Apoptosis-inducing Ligand in *FGFR3*-mutated Tumors, Eur Urol (2023), https://doi.org/10.1016/j.eururo.2023.05.037

2.2. Proteomic quantification and analyses

Proteome was quantified using the super-SILAC method and an LC-MS/MS analysis. Proteomic data were initially explored using a principal component analysis (PCA), followed by clustering using ConsensusClusterPlus. Identified unsupervised protein groups (uPGs) were compared with the transcriptomic NMIBC [15] and MIBC subtypes [16]; characterized using a protein expression differential analysis, a gene set enrichment analysis (GSEA) pathway enrichment analysis, asso-

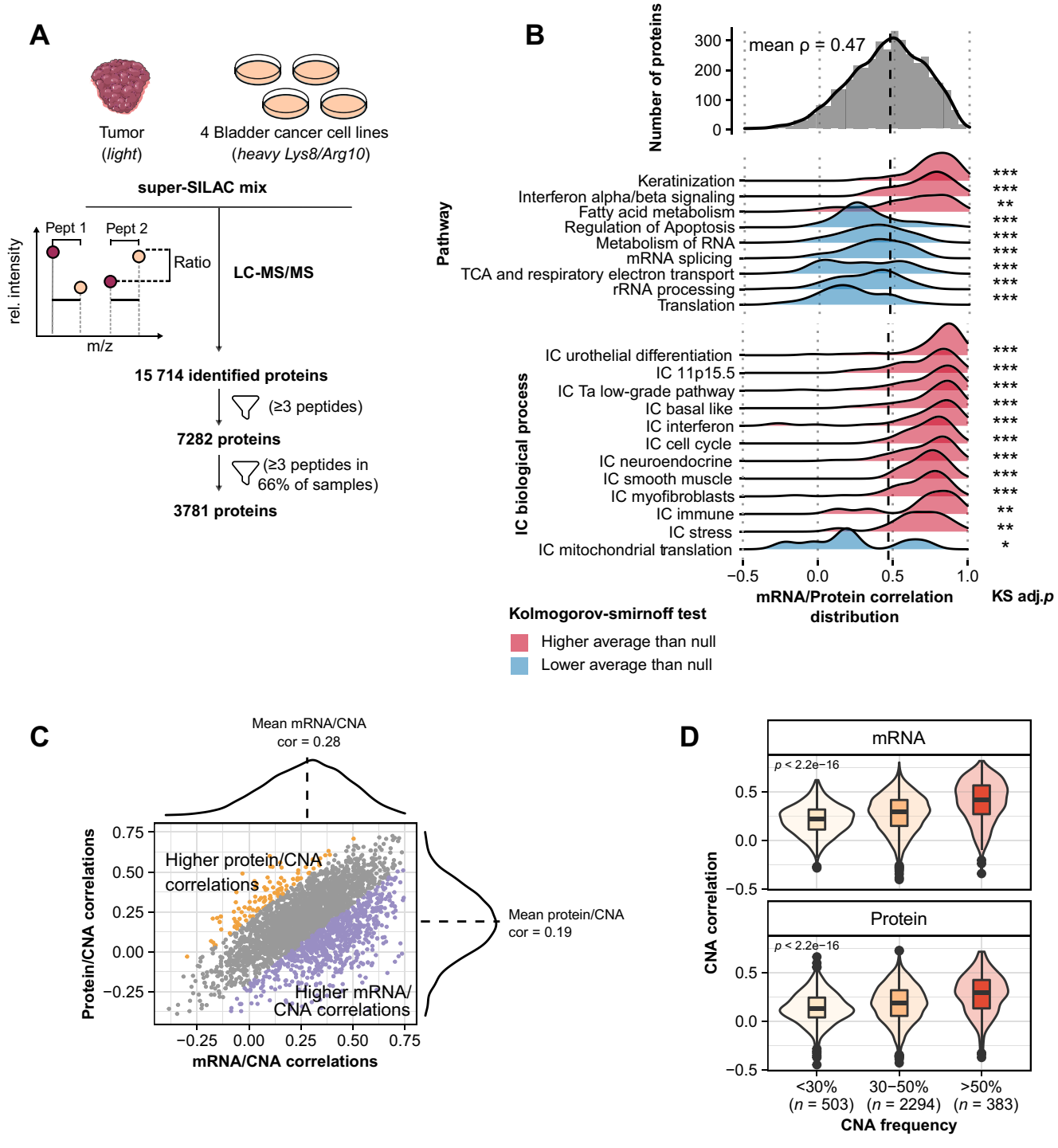

Fig. 1 – Workflow for proteomic data acquisition and correlation between omic data. (A) Diagram of super-SILAC mass spectrometry workflow. Protein quantities were given as ratios between the light (tumor) and heavy (four cell lines) versions of peptides (see the Supplementary material). (B) Density plots of mRNA/protein Spearman correlations: overall density of mRNA/protein correlations (top), for selected pathways from the Reactome Pathway Database (center), and for transcriptomic independent components identified by Biton et al [28] (bottom). Kolmogorov-Smirnoff adjusted p values are as follows: *** p < 0.001, ** p < 0.01, and * p < 0.05 (Supplementary Table 2). (C) The mRNA/CNA and protein/CNA correlations. Orange and purple points have significantly higher protein/CNA and mRNA/CNA correlations (adj. p < 0.05), respectively. The distributions of the mRNA/CNA and protein/CNA correlations are shown as distribution plots in the upper and right margins, respectively, and the mean of each distribution (cor). (D) Violin/box plots comparing the distributions of CNA/mRNA (top) and CNA/protein correlations (bottom) by estimated frequency of copy number aberrations per gene using Kruskal-Wallis tests. CNA = copy number alteration; IC = independent component; LC-MS/MS = liquid chromatography coupled to tandem mass spectrometry; rel. intensity = relative intensity.

Please cite this article as: C.S. Groeneveld, V. Sanchez-Quiles, F. Dufour et al., Proteogenomic Characterization of Bladder Cancer Reveals Sensitivity to Apoptosis Induced by Tumor Necrosis Factor–related Apoptosis-inducing Ligand in *FGFR3*-mutated Tumors, Eur Urol (2023), https://doi.org/10.1016/j.eururo.2023.05.037

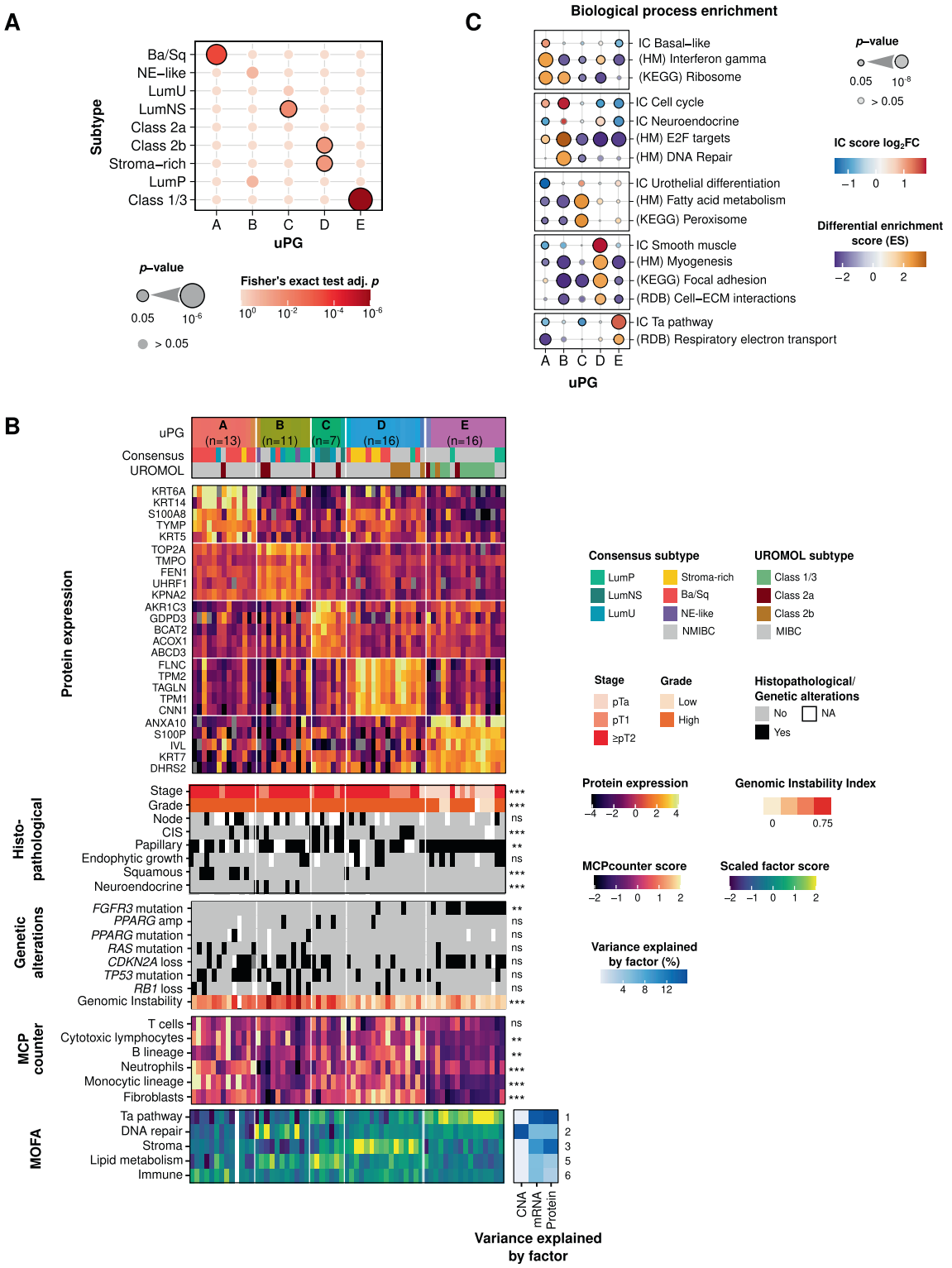

Fig. 2 – Analysis of unsupervised proteomic groups (uPGs). (A) Comparison of uPGs and transcriptomic subtypes. Point size and color represent *p* values calculated by Fisher's exact tests, adjusted using the Benjamini-Hochberg method. (B) Characterization of tumors within each uPG. Bladder tumors were clustered into five groups: uPG-A, uPG-B, uPG-C, uPG-D, and uPG-E (see Supplementary Fig. 3). The uPGs were described according to transcriptomic subtype, most differentially expressed proteins, clinical and histopathological variables, selected common genetic alterations, MCPcounter scores measuring the abundance of microenvironment cell population, and multiomic factor (MOFA) scores (see also Supplementary Fig. 5). Variance explained by MOFA factors in each omic is presented to the right of the MOFA score panel. Within each uPG, samples were ordered by clustering based on MOFA scores. (C) Main biological processes enriched for each uPG. Biological processes derived from the transcriptomic IC analysis or curated annotated databases: KEGG, Reactome Database (RDB), and MSigDB Hallmarks (HM). Ba/Sq = basal/squamous; CNA = copy number alteration; ECM = extracellular matrix; IC = independent component; LumNS = luminal nonspecified; LumP = luminal papillary; LumU = luminal unstable; MIBC = muscle-invasive bladder cancer; NE = neuroendocrine; NMIBC = non–muscle-invasive bladder cancer.

Please cite this article as: C.S. Groeneveld, V. Sanchez-Quiles, F. Dufour et al., Proteogenomic Characterization of Bladder Cancer Reveals Sensitivity to Apoptosis Induced by Tumor Necrosis Factor–related Apoptosis-inducing Ligand in *FGFR3*-mutated Tumors, Eur Urol (2023), https://doi.org/10.1016/j.eururo.2023.05.037

ciation with histopathological features, genomic alterations, and a multiomic factor analysis (MOFA); and validated using two independent proteomic series [25,26].

Pathways potentially activated in *FGFR3*-mutated tumors were identified based on the GSEA analysis of differentially expressed genes/proteins between *FGFR3*-mutated and *FGFR3* wild-type tumors.

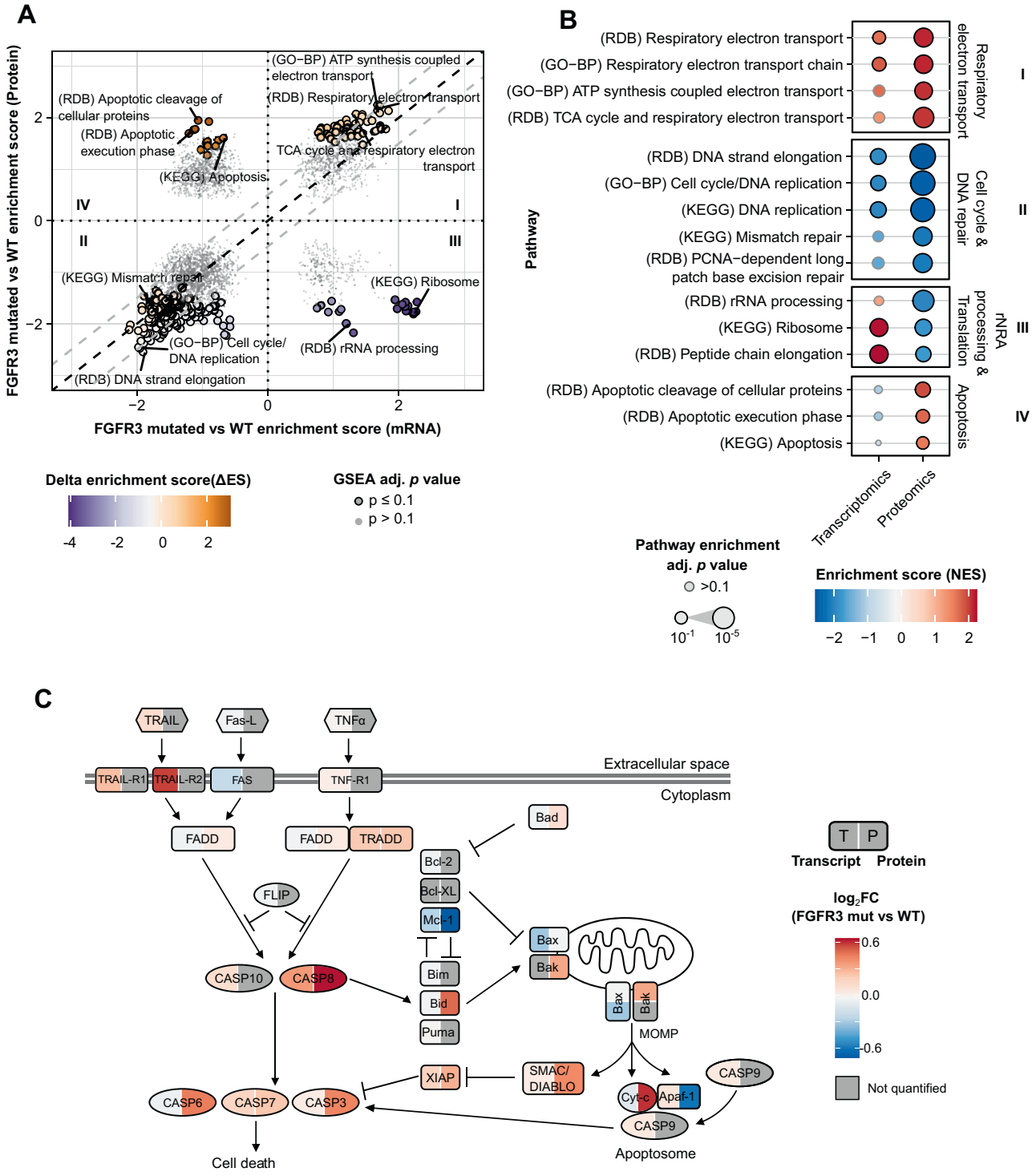

Fig. 3 – Proteomic analysis of *FGFR3*-mutated tumors reveals new pathways potentially activated in these tumors. (A) Pathway enrichment scores of *FGFR3*-mutated versus *FGFR3* wild-type tumors derived from either proteomic (*y* axis) or transcriptomic (*x* axis) data. Pathways significantly enriched (adj. $p \leq 0.1$) are represented as circles with black outline and nonsignificantly enriched as grey dots. Delta enrichment scores (ΔES), calculated as the difference between protein and mRNA enrichment scores, are encoded by point colors. Annotated circle labels were manually curated from pathways with significant ΔES. (B) Enrichment scores and significance of selected pathways derived from transcriptomic or proteomic data. Pathways selected from those shown as significant in Figure 3A and grouped according to quadrant, highlighting similarities (quadrants I and II) or differences (quadrants III and IV) between transcriptomic and proteomic ES. (C) Visualization of the apoptosis pathway (adapted from the KEGG apoptosis pathway), with transcriptomic (left) and proteomic (right) log fold-change between *FGFR3*-mutated and WT tumors overlayed as color. NES = normalized enrichment score; RDB = Reactome Database; WT = wild type.

Please cite this article as: C.S. Groeneveld, V. Sanchez-Quiles, F. Dufour et al., Proteogenomic Characterization of Bladder Cancer Reveals Sensitivity to Apoptosis Induced by Tumor Necrosis Factor–related Apoptosis-inducing Ligand in *FGFR3*-mutated Tumors, Eur Urol (2023), https://doi.org/10.1016/j.eururo.2023.05.037

Nonparametric tests were used for comparisons (Kruskal-Wallis for multiple groups and Wilcoxon rank-sum for two groups). Kolmogorov-Smirnoff tests were used to compare subsets with the overall distribution of CNA/protein, CNA/mRNA, and mRNA/protein correlations. One-sample *t* tests and Fisher exact tests were used when appropriate. Reported *p* values are adjusted using the Benjamini-Hochberg method with a false discovery rate of 5% unless otherwise specified.

2.3. Functional experiments

Pharmacological and knockdown experiments were performed as described in the Supplementary material.

3. Results

3.1. Proteome quantification and correlation between omic data in bladder tumors

We profiled the proteome of 23 NMIBC and 40 MIBC cases from the Carte d'Identité des Tumeurs (CIT) series, previously characterized at the transcriptomic and genomic levels [11,28]. This multiomic characterization was performed on the same fresh frozen tissue samples, thanks to a triple extraction method [29]. We selected 63 tumors from all the different transcriptomic subtypes according to the UROMOL 2021 classification for NMIBC and the consensus classification for MIBC, while maintaining the proportions of subtypes found in larger cohorts [15,16]. The clinical, histopathological, and molecular data are shown in Supplementary Table 1. We quantified the proteome using a super-SILAC strategy, where a common heavy-labeled internal reference from a mix of cell lines allows for accurate comparisons of protein ratios between tumors (Fig. 1A) [30]. We quantified 15 714 proteins and kept 3781 proteins including only those identified by three or more different peptides in ≥66% of samples (Fig. 1A, and Supplementary Fig. 1A and 1B). These 3781 filtered proteins represented the whole proteome diversity, as shown by their wide-ranging isoelectric point, molecular weight, and solubility (Supplementary Fig. 1C). They had the expected dynamic range of protein functions and were localized in diverse subcellular compartments (Supplementary Fig. 1D and 1E).

We examined the correlation across tumors between mRNA and protein expression (Fig. 1B and Supplementary Table 2). Overall, 90.1% of the mRNA/protein pairs showed a significant positive correlation (adj. $p < 0.05$). The mean Spearman correlation coefficient we obtained ($\rho = 0.47$; Fig. 1B, upper panel) was within the range reported in previous studies (0.39–0.53) [20–24]. The mRNA/protein correlations can differ significantly depending on the biological processes [21,23,24]. This was also observed in our series considering Reactome Pathway Database gene sets (Fig. 1B, middle panel). We also investigated the biological processes that we previously identified in bladder cancer

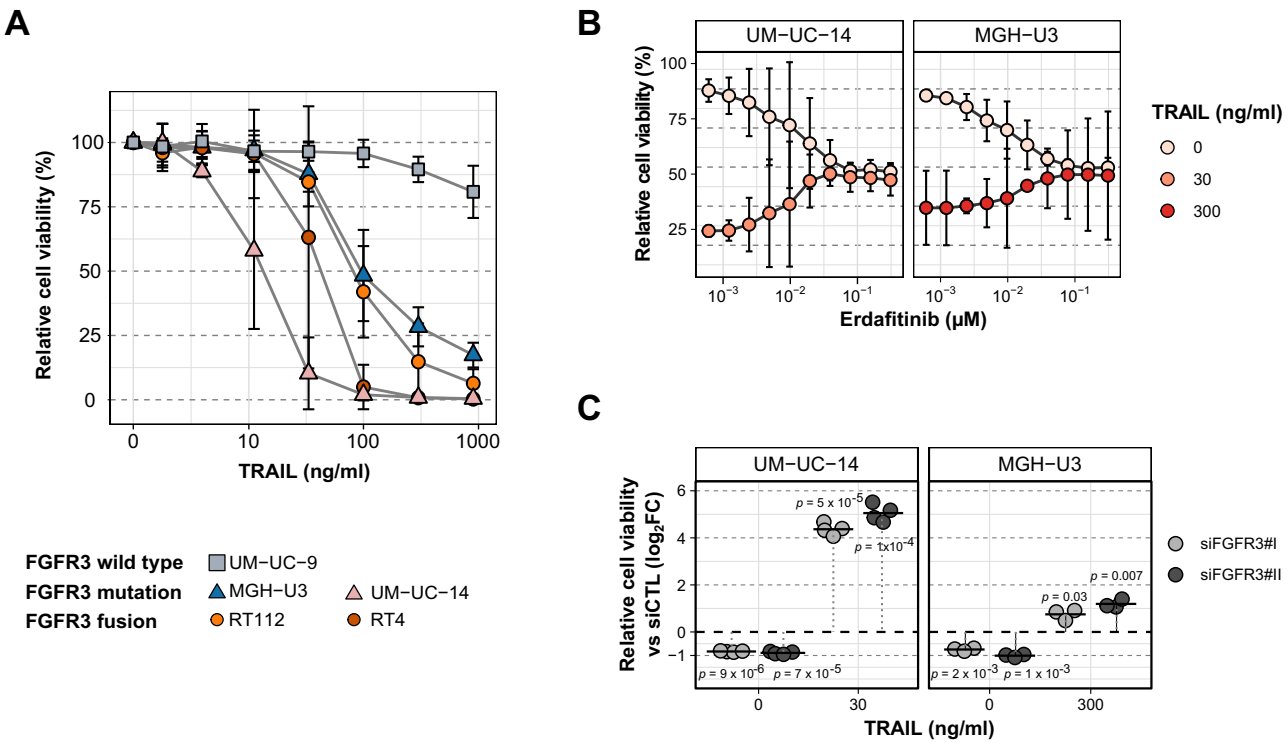

Fig. 4 – FGFR3 activation through genetic alterations sensitizes urothelial bladder cancer cell lines to TRAIL. (A) Cell viability (CellTiter-Glo assay) for indicated cell lines (four FGFR3-altered ones and UMUC9) treated with 0–1000 ng/ml TRAIL for 24 h. Error bars indicate 95% CI ($n = 3$). (B) Cell viability for UM-UC-14 and MGH-U3 cells treated with increasing concentrations of erdafitinib for 24 h and treated for an additional 24 h with TRAIL at indicated concentrations. Error bars indicate 95% CI ($n = 3$). (C) Cell viability for UM-UC-14 and MGH-U3 cells transfected with siRNA control (siCTL) or *FGFR3* siRNA (siFGFR3#I or siFGFR3#II) for 48 h, then treated with TRAIL for 24 h. Results were compared with baseline cell viability using one-sample *t* tests (unadjusted *p* values). CI = confidence interval; TRAIL = tumor necrosis factor–related apoptosis-inducing ligand.

Please cite this article as: C.S. Groeneveld, V. Sanchez-Quiles, F. Dufour et al., Proteogenomic Characterization of Bladder Cancer Reveals Sensitivity to Apoptosis Induced by Tumor Necrosis Factor–related Apoptosis-inducing Ligand in *FGFR3*-mutated Tumors, Eur Urol (2023), https://doi.org/10.1016/j.eururo.2023.05.037

using an independent component (IC) analysis from transcriptomic data (Fig. 1B, lower panel) [28], and found high correlations for mRNA/protein most associated with ICs.

Next, we examined the effects of copy number alterations (CNAs) on mRNA and protein levels (Fig. 1C and 1D, Supplementary Table 3, and Supplementary material). The mRNA/CNA correlations were significantly higher (KS test $p < 10^{-15}$) than the protein/CNA correlations (Fig. 1C), in agreement with previous findings in other cancers [19,24]. In addition, higher correlations were found for genes presenting the highest frequency of genomic alterations (Fig. 1D).

3.2. Identification and characterization of bladder tumor proteomic groups

We first performed a PCA of the filtered proteomic data of the 63 tumors (Supplementary Fig. 2 and Supplementary Table 4). Lower values of PC1 were associated with high expression of proteins of the microenvironment and immune- and/or stroma-infiltrated tumors (NMIBC class 2b, MIBC basal tumors, and stroma-rich tumors). Lower values of PC2 were associated with high expression of proliferation markers and most MIBC basal, luminal unstable, and neuroendocrine-like tumors.

We then performed unsupervised consensus clustering of the 63 tumors on the filtered proteomic data. Five uPGs (A–E) emerged (Supplementary Fig. 3A–C). The uPGs showed coarse-grained similarities to transcriptomic NMIBC and MIBC subtypes (Fig. 2A and 2B [top panel] and Supplementary Fig 3D). We characterized the uPGs according to protein expression data, clinical and histopathological characteristics, common bladder cancer genetic alterations, and biological process enrichment (Fig. 2B and 2C, Supplementary Table 5, and Supplementary Fig. 4A). Altogether, uPG-A was enriched in Ba/Sq tumors and overexpressed basal markers; uPG-B was highly heterogeneous but grouped tumors with high expression of cell cycle and DNA repair proteins; uPG-C was related to luminal nonspecified tumors; uPG-D, which displayed enrichment of proteins and pathways related to smooth muscle and extracellular matrix, was enriched in both NMIBC class 2b and MIBC stroma-rich tumors, and contained the remaining Ba/Sq tumors; and uPG-E, strongly enriched in class 1/3 NMIBC samples, was also enriched in proteins corresponding to the transcriptomic IC Ta pathway. Accordingly, it contained all but one of the pTa tumors and most of the *FGFR3*-mutated tumors. Using an mRNA-based microenvironment cell population estimation tool (MCPcounter) [31], we also found that the uPGs differed in the expression of markers of multiple microenvironment cell populations (Fig. 2B [MCP panel] and Supplementary Fig. 4B) and in the expression of PD-L1 (Supplementary Fig. 4C).

To further characterize our series, we used a MOFA [32] to jointly reduce the dimensionality of the three omic data types. We identified ten MOFA factors and could biologically interpret five of them (factor 1: Ta pathway; 2: DNA repair; 3: stroma; 5: lipid metabolism; and 6: immune; Supplementary Fig. 5, Supplementary Table 6, and Supplementary material). The DNA repair, lipid metabolism, stroma, and Ta pathway factors were associated with uPG-B, uPG-C, uPG-D, and uPG-E, respectively (Fig. 2B, MOFA panel); uPG-B also presented the highest levels of genomic instability (Fig. 2B, genetic alterations panel), as expected given its association with the DNA repair factor.

Stroggilos et al [25] performed label-free proteomic quantification of 1515 proteins in a cohort of 98 NMIBC and 19 MIBC cases, and identified three NMIBC proteomic subtypes (NPS1–3). We developed a classifier of NPS1–3 from their data and applied it to our bladder cancer series (Supplementary material). We found a strong correspondence between NPS2 and NPS3 with uPG-D and uPG-E, respectively, with a close overlap of the overexpressed proteins (Supplementary Fig. 6A). We further compared our uPGs with the label-free proteomic quantifications from formalin-fixed paraffin-embedded samples in the study by Xu et al [26], who reported three proteome clusters incorporating both NMIBC and MIBC (from U-I to U-III; Supplementary Fig. 6B and 6C). In the data of Xu et al's [26] study, uPG-E corresponded to a subset of U-I and contained almost all *FGFR3*-mutated tumors ($p = 0.001$), U-II tumors displayed high expression of uPG-B markers spanning both NMIBC and MIBC, and U-III corresponded to both uPG-A and uPG-D tumors. Thus, despite using distinct proteomic methods and source material, both datasets showed strong concordance with four out of the five uPGs (uPG-A, uPG-B, uPG-D, and uPG-E).

3.3. Proteomic analyses highlight potential roles of mutated FGFR3 in apoptosis in bladder cancer

To better characterize the biology of *FGFR3*-mutated tumors, we compared them with wild-type (WT) *FGFR3* tumors at the proteome and transcriptome levels. We calculated pathway enrichment scores using GSEA from proteomic and transcriptomic fold-change values between *FGFR3*-mutated and WT tumors (Supplementary Table 7). Most of the statistically significant pathways (231/269) presented similarly positive or negative enrichment scores in both proteomic and transcriptomic data, with the remaining 38 pathways showing opposite enrichments (Fig. 3A). Three biological processes related to apoptosis were significantly positively enriched, specifically in the proteomic data, in *FGFR3*-mutated tumors compared with WT tumors (Fig. 3A and 3B [quadrant IV]). We thus focused on the apoptosis pathway (Fig. 3C). At the protein level, we observed differences between *FGFR3*-mutated and WT tumors that were less or not apparent by a transcriptome analysis, most notably for the initiator caspase-8 and its effector, BID, as well as the apoptosis effectors caspase-3 and caspase-6, which were all upregulated at the protein level in *FGFR3*-mutated tumors. This proteomic-based observation suggested that tumor cells harboring *FGFR3* mutations could be particularly sensitive to proapoptotic stimuli. One such stimulus could include the tumor necrosis factor–related apoptosis-inducing ligand (TRAIL), since at the transcriptomic level, *FGFR3*-mutated tumors showed higher gene expression of both *TNFRSF10A* and *TNFRSF10B*, encoding for TRAIL receptors TRAIL-R1 and TRAIL-R2, respectively (Fig. 3C and Supplementary Table 7).

Please cite this article as: C.S. Groeneveld, V. Sanchez-Quiles, F. Dufour et al., Proteogenomic Characterization of Bladder Cancer Reveals Sensitivity to Apoptosis Induced by Tumor Necrosis Factor–related Apoptosis-inducing Ligand in *FGFR3*-mutated Tumors, Eur Urol (2023), https://doi.org/10.1016/j.eururo.2023.05.037

3.4. Tumor cell lines harboring genetic alterations of FGFR3 are sensitive to TRAIL-mediated apoptosis

Various susceptibilities of urothelial cancer cell lines to TRAIL have been reported [33–35], though the link with *FGFR3* alteration status was never previously assessed. Here, we evaluated sensitivity to TRAIL in five cell lines, four harboring genetic alterations of *FGFR3* (mutations for UM-UC-14 and MGH-U3; *FGFR3-TACC3* fusions for RT112 and RT4), and one presenting WT *FGFR3*, already shown to be resistant to TRAIL (UM-UC-9) [35], used as a negative control (Fig. 4A). In line with our hypothesis, all *FGFR3*-altered cell lines were sensitive to TRAIL. To validate a relationship between *FGFR3* activation and sensitivity to TRAIL, we pretreated UM-UC-14 and MGH-U3 cells with erdafitinib, a pan-*FGFR* inhibitor (Fig. 4B), or *FGFR3* siRNA (Fig. 4C) prior to treatment of the cells with TRAIL. These pretreatments significantly dampened the impact of TRAIL treatment on cell viability, demonstrating that the sensitivity to TRAIL of *FGFR3*-mutated cell lines depends on FGFR3 expression.

3.5. FGFR3 activation favors accumulation of TRAIL receptors and inhibition of c-FLIP

To gain insight into the mechanism of *FGFR3*-mediated sensitization to TRAIL, we assessed expression levels of key genes within the death receptor pathway after *FGFR3* knockdown by siRNA using our previously obtained transcriptomic data in UM-UC-14, RT112, and MGH-U3 cells (Fig. 5A) [36,37]. We observed decreased expression of *TNFRSF10A*, encoding TRAIL-R1, whereas the expression of *CFLAR*, encoding the pro-caspase-8/-10 inhibitor c-FLIP, known to regulate sensitivity to TRAIL-induced apoptosis in urothelial tumor cells [33], was increased (Stouffer aggregated $p = 0.00001$ and 0.001, respectively). Accordingly, we observed a decrease of TRAIL-R1 and an increase of c-FLIP at the protein level, after *FGFR3* knockdown (Fig. 5B) and FGFR3 inhibition using erdafitinib (Fig. 5C) in UM-UC-14 and MGH-U3 cells. Of note, although not significant at the mRNA level (Fig. 5A), we also observed a slight decrease in TRAIL-R2 protein levels after FGFR3 modulation (Fig. 5B and 5C). In agreement, we observed the upregulation of

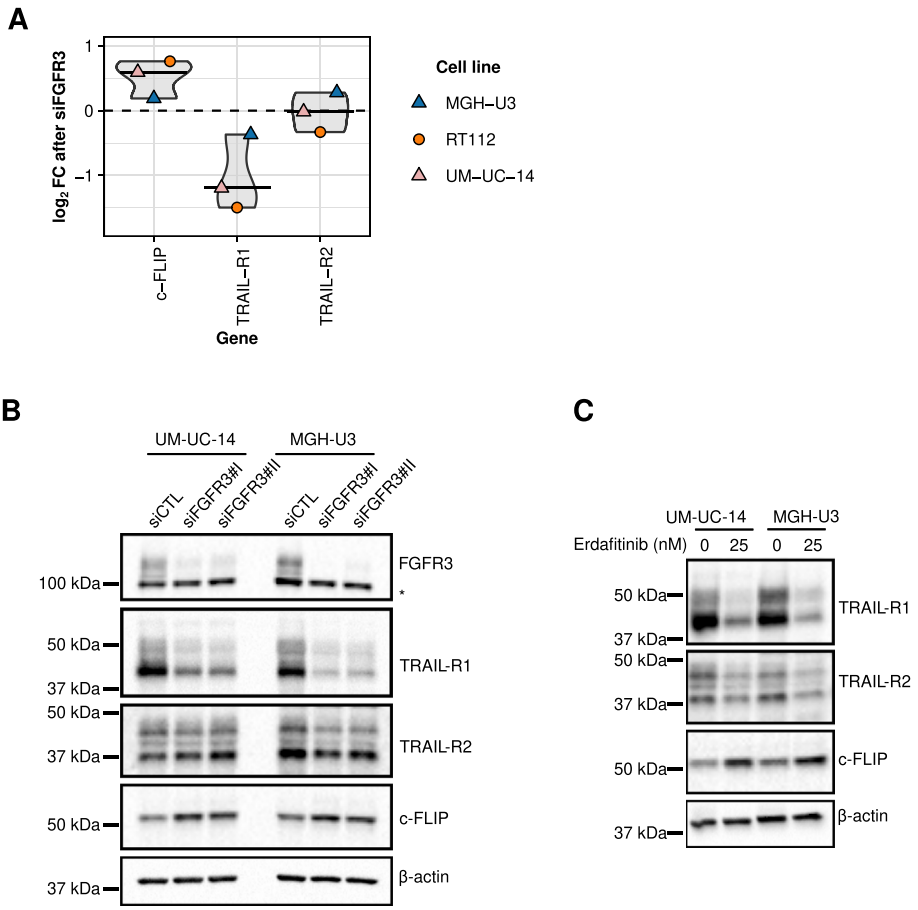

Fig. 5 – FGFR3 activation through genetic alterations induces accumulation of TRAIL receptors and loss of c-FLIP. (A) Gene expression level assessed by Affymetrix array (U133plus2.0) of TRAIL-mediated apoptosis pathway players *CFLAR* (encoding c-FLIP), *TNFRSF10A* (encoding TRAIL-R1), and *TNFRSF10B* (encoding TRAIL-R2) after FGFR3 knockdown using siRNA in MGH-U3, RT112, and UM-UC-14. Data were obtained from previous studies from our group [36,37]. Western blotting of TRAIL-R1, TRAIL-R2, and c-FLIP in UM-UC-14 and MGH-U3 cells (B) transfected with indicated siRNA for 48 h or (C) treated with erdafitinib or DMSO control for 24 h. Blots are representative results of three independent experiments. DMSO = dimethylsulfoxide; TRAIL = tumor necrosis factor–related apoptosis-inducing ligand.

Please cite this article as: C.S. Groeneveld, V. Sanchez-Quiles, F. Dufour et al., Proteogenomic Characterization of Bladder Cancer Reveals Sensitivity to Apoptosis Induced by Tumor Necrosis Factor–related Apoptosis-inducing Ligand in *FGFR3*-mutated Tumors, Eur Urol (2023), https://doi.org/10.1016/j.eururo.2023.05.037

Tnfrsf10b in our *FGFR3*-induced bladder cancer model in mice [38]. Taken together, our results indicate that *FGFR3* activation through genetic alterations confers sensitivity to TRAIL-induced apoptosis by favoring the accumulation of TRAIL-agonistic receptors with concomitant inhibition of c-FLIP, the main caspase-8/10 endogenous inhibitor.

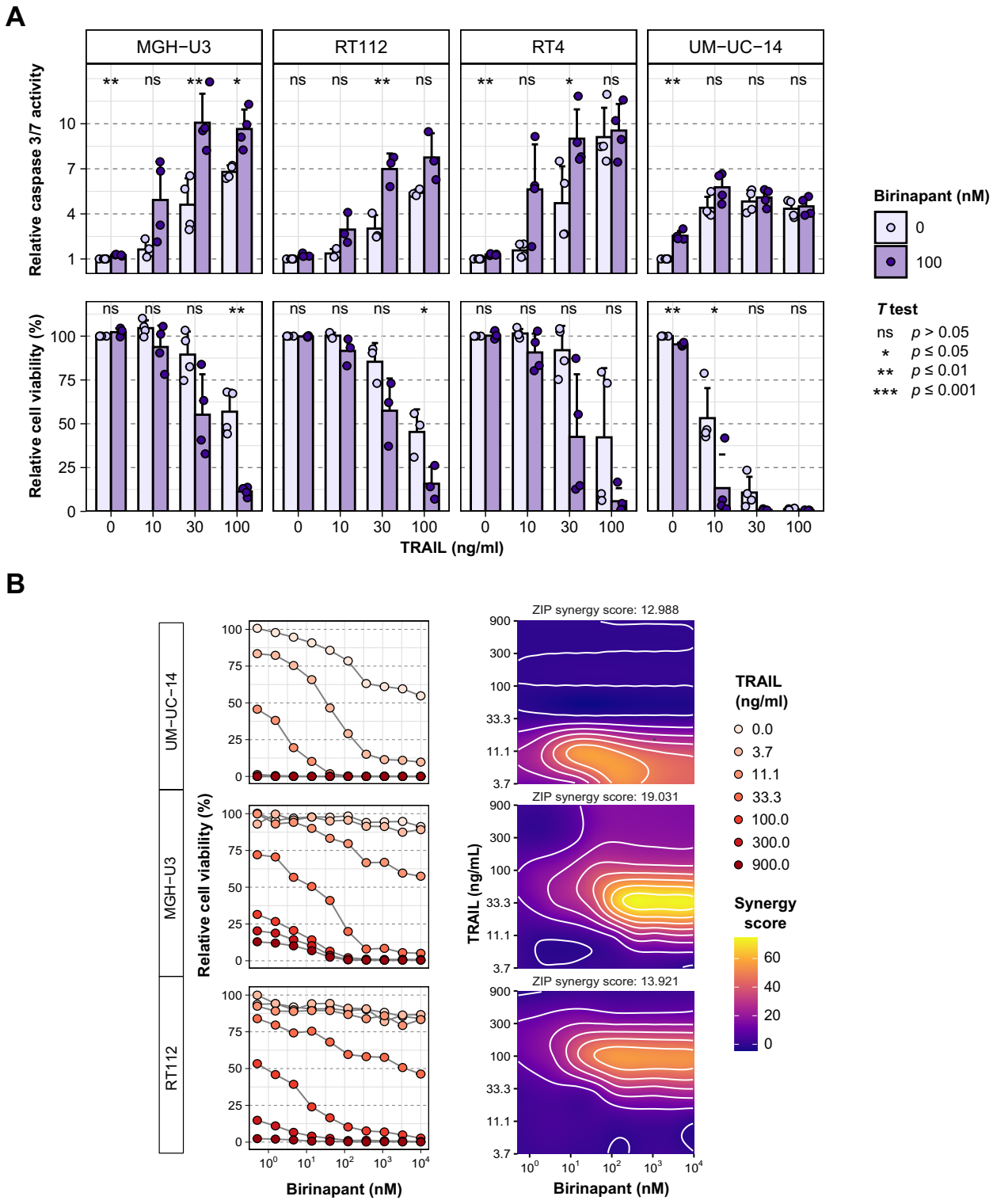

Fig. 6 – Combination of TRAIL with apoptotic sensitizer birinapant is synergistic in *FGFR3*-altered urothelial cell lines. (A) Apoptosis (top) measured by casp3/7Glo assay and cell viability (bottom) measured by CellTiterGlo for four *FGFR3*-altered cell lines treated with TRAIL in combination with birinapant for 24 h. Samples treated with the birinapant/TRAIL combination were compared with samples treated only with TRAIL using Welch's *t* tests. Error bars indicate standard deviation ($n = 4$). (B) Representative examples of a TRAIL dose-response in combination with birinapant. Indicated FGFR3-altered cells were treated for 72 h with indicated concentrations of birinapant and/or TRAIL. Cell viability was measured by the CellTiter-Glo assay (left panels), and drug combination response was calculated based on the zero interaction potency (ZIP) model using SynergyFinder (right panels). The mean ZIP synergy scores are indicated. ns = nonsignificant; TRAIL = tumor necrosis factor–related apoptosis-inducing ligand.

Please cite this article as: C.S. Groeneveld, V. Sanchez-Quiles, F. Dufour et al., Proteogenomic Characterization of Bladder Cancer Reveals Sensitivity to Apoptosis Induced by Tumor Necrosis Factor–related Apoptosis-inducing Ligand in *FGFR3*-mutated Tumors, Eur Urol (2023), https://doi.org/10.1016/j.eururo.2023.05.037

3.6. Birinapant synergizes with TRAIL to decrease cell viability in FGFR3-altered cell lines

The members of the inhibitor of apoptosis protein (IAP) family, including *XIAP*, are also negative regulators of caspase activation and can be inhibited by the second mitochondrial-derived activator of caspases (SMAC). Combining SMAC peptidomimetics, such as birinapant, with TRAIL has been identified as an efficient TRAIL-sensitizing strategy in several models [39]. Notably, SMAC was also highly upregulated at the protein level in our *FGFR3*-mutated tumors (Fig. 3C). We, therefore, evaluated the impact of recombinant TRAIL in combination with birinapant in our four *FGFR3*-altered bladder cancer cell lines. We observed an increase in apoptosis, measured through caspase-3/7 activity (Fig. 6A, top panel), and a concomitant decrease in cell viability (Fig. 6A, bottom panel) in the presence of both drugs as compared to single treatments. We further characterized the combination of the two drugs by treating UM-UC-14, MGH-U3, and RT112 cell lines with increasing concentrations of each drug (Fig. 6B, left panel) and used these results to calculate synergy scores using the zero interaction potency (ZIP) model (Fig. 6B, right panel). The addition of birinapant resulted in synergistic sensitization to TRAIL in all three cell lines (ZIP score >10). Altogether, we conclude that apoptosis is efficiently induced by TRAIL in *FGFR3*-altered bladder cancer cells and SMAC inhibition represents a promising treatment combination.

4. Discussion

Our proteomic classification demonstrated coarse-grained similarities with transcriptomic-derived NMIBC and MIBC subtyping, but also revealed heterogeneity within transcriptomic subtypes. Further exploring the heterogeneity of NMIBC subtype 2a, highlighted by our proteomic analysis, is of clinical interest, as this subtype has been shown to be the most aggressive of the NMIBC subtypes [15]. Likewise, considering the heterogeneity of basal tumor microenvironments could be of interest for improving immunotherapy treatments. While our proteomic analysis showed the heterogeneity of several transcriptomic subtypes, the proteome enabled the grouping of tumors that differed in transcriptomic classification but shared common features, as exemplified by uPG-B tumors, which shared high proliferation and genomic instability. These clues could lead to common treatments for these tumors.

Our proteogenomic analyses also highlighted a higher abundance of apoptosis proteins in *FGFR3*-mutated tumors, which had not been reported previously. Our functional *in vitro* experiments identified TRAIL treatment as a promising therapeutic strategy for *FGFR3*-altered bladder tumors. These results are of particular interest given that pan-*FGFR* inhibitors are limited by the rapid emergence of resistance [8]. As clinical use of SMAC mimetics, such as birinapant, raised safety concerns due to cytokine-release syndrome [40,41], intravesical instillation would provide a safe and efficient strategy to combine birinapant with TRAIL-based proapoptotic agents for *FGFR3*-mutated NMIBC (which represent approximately 70% of NMIBC cases). Investigations to extend TRAIL treatment strategies to *FGFR3*-altered tumors in other cancers would be of interest since multiple myeloma cell lines OPM-2 and KMS-11, harboring *FGFR3* mutations, are highly sensitive to TRAIL [42].

Our work has some limitations. The number of samples was relatively small (23 NMIBC and 40 MIBC cases); however, this limitation was partly circumvented by using validation cohorts with proteomic data. Additional multiomic studies including proteomic data are still warranted in bladder cancer. We noted that some non–*FGFR3*-mutated tumors respond to TRAIL [33–35], but the mechanisms involved have still to be identified to be able to select the non–*FGFR3*-mutated cancers that could also respond to a TRAIL-based treatment.

5. Conclusions

This study provides a proteomic, genomic, and transcriptomic resource for NMIBC and MIBC investigation. It bolsters and refines existing classifications of bladder tumors and identifies potential subtype protein markers that pave the way for future immunohistochemical subtyping that could easily be implemented in clinical practice. Based on new insights underlying *FGFR3*-mutated tumors, we demonstrated that *FGFR3* alterations confer sensitivity to TRAIL-induced apoptosis, which can be potentialized using sensitizers such as birinapant. In the clinic, anti-FGFR treatment has shown clear benefits for patients with *FGFR3*-mutated bladder cancer, but treatment resistance is a major challenge. Therefore, the alternative approach proposed here warrants further clinical investigation.

***Author contributions*:** François Radvanyi had full access to all the data in the study and takes responsibility for the integrity of the data and the accuracy of the data analysis.

Study concept and design: Groeneveld, Sanchez-Quiles, Dufour, Micheau, Bernard-Pierrot, Radvanyi.
Acquisition of data: Sanchez-Quiles, Dufour, Shi, Dingli, Poullet, Krucker, Maillé, Vacherot, Vordos, Benhamou, Lebret, Allory.
Analysis and interpretation of data: Groeneveld, Sanchez-Quiles, Dufour, Nicolle, Chapeaublanc, Allory, de Reyniès, Bernard-Pierrot, Radvanyi.
Drafting of the manuscript: Groeneveld, Sanchez-Quiles, Dufour, Jeffery.
Critical revision of the manuscript for important intellectual content: Jeffery, Allory, de Reyniès, Bernard-Pierrot, Radvanyi.
Statistical analysis: Groeneveld, Dufour, Nicolle, Chapeaublanc.
Obtaining funding: Allory, de Reyniès, Bernard-Pierrot, Radvanyi.
Administrative, technical, or material support: Dingli, Chapeaublanc, Vacherot, Loew.
Supervision: Allory, de Reyniès, Bernard-Pierrot, Radvanyi.
Other: methodology: Groeneveld, Sanchez-Quiles, Dufour, Nicolle, Zinovyev, Loew, de Reyniès, Bernard-Pierrot, Radvanyi; software: Groeneveld.

Financial disclosures: François Radvanyi certifies that all conflicts of interest, including specific financial interests and relationships and affiliations relevant to the subject matter or materials discussed in the manuscript (eg, employment/affiliation, grants or funding, consultancies,

Please cite this article as: C.S. Groeneveld, V. Sanchez-Quiles, F. Dufour et al., Proteogenomic Characterization of Bladder Cancer Reveals Sensitivity to Apoptosis Induced by Tumor Necrosis Factor–related Apoptosis-inducing Ligand in *FGFR3*-mutated Tumors, Eur Urol (2023), https://doi.org/10.1016/j.eururo.2023.05.037

honoraria, stock ownership or options, expert testimony, royalties, or patents filed, received, or pending), are the following: None.

***Funding/Support and role of the sponsor*:** This work was supported by the Carte d'Identité des Tumeurs (CIT) program from La Ligue Nationale Contre le Cancer (LNCC), by the Institut National Contre le cancer (INCa; PLBio2005-039 and PRTK2007-UROPATH, 2013-1-RT-01), by a grant of the LNCC to Clarice S. Groeneveld, Virginia Sanchez-Quiles, Florent Dufour, Mingjun Shi, Elodie Chapeaublanc, Clémentine Krucker, Yves Allory, Isabelle Bernard-Pierrot, and François Radvanyi as an associated team (Equipe Labellisée). Virginia Sanchez-Quiles was supported by a grant from the LNCC. Mingjun Shi was supported by the National Natural Science Foundation of China (NSFC; 82002672).

***Data sharing*:** LC-MS raw data are available through PRIDE under accession number PXD022435. Copy number alteration data are available on GEO under accession number GSE198328. Processed data are freely available on GitHub (https://github.com/csgroen/cit_blca_proteomics/tree/main/analysis/data). All relevant codes used for analyses and generation of figures are available on GitHub (https://github.com/csgroen/cit_blca_proteomics). A docker image of the R analysis environment is also provided to ensure reproducibility.

***Acknowledgments*:** We would like to thank Olivier Ayrault, Antoine Forget, and Emmanuel Barillot for their valuable suggestions and advice on proteomics analysis.

Peer Review Summary

Peer Review Summary and Supplementary data to this article can be found online at https://doi.org/10.1016/j.eururo.2023.05.037.

References

[1] Netto GJ, Amin MB, Berney DM, et al. The 2022 World Health Organization classification of tumors of the urinary system and male genital organs: prostate and urinary tract tumors. Eur Urol 2022;82:469–82.
[2] Lopez-Beltran A, Cimadamore A, Montironi R, Cheng L. Molecular pathology of urothelial carcinoma. Hum Pathol 2021;113:67–83.
[3] Billerey C, Chopin D, Aubriot-Lorton M-H, et al. Frequent FGFR3 mutations in papillary non-invasive bladder (pTa) tumors. Am J Pathol 2001;158:1955–9.
[4] Robertson AG, Kim J, Al-Ahmadie H, et al. Comprehensive molecular characterization of muscle-invasive bladder cancer. Cell 2017;171:540–556.e25.
[5] Babjuk M, Burger M, Capoun O, Cohen D, et al. European Association of Urology guidelines on nonmuscle-invasive bladder cancer (Ta, T1, and carcinoma in situ). Eur Urol 2022;81:75–94.
[6] Witjes JA, Bruins HM, Cathomas R, et al. European Association of Urology guidelines on muscle-invasive and metastatic bladder cancer: summary of the 2020 guidelines. Eur Urol 2021;79:82–104.
[7] Powles T, Bellmunt J, Comperat E, et al. Bladder cancer: ESMO clinical practice guideline for diagnosis, treatment and follow-up. Ann Oncol 2022;33:244–58.
[8] Loriot Y, Necchi A, Park SH, et al. Erdafitinib in locally advanced or metastatic urothelial carcinoma. N Engl J Med 2019;381:338–48.
[9] Choi W, Porten S, Kim S, Willis D, et al. Identification of distinct basal and luminal subtypes of muscle-invasive bladder cancer with different sensitivities to frontline chemotherapy. Cancer Cell 2014;25:152–65.
[10] Damrauer JS, Hoadley KA, Chism DD, et al. Intrinsic subtypes of high-grade bladder cancer reflect the hallmarks of breast cancer biology. Proc Natl Acad Sci U S A 2014;111:3110–5.
[11] Rebouissou S, Bernard-Pierrot I, De Reyniès A, et al. EGFR as a potential therapeutic target for a subset of muscle-invasive bladder cancers presenting a basal-like phenotype. Sci Transl Med 2014;6:244ra91.
[12] Hurst CD, Alder O, Platt FM, et al. Genomic subtypes of non-invasive bladder cancer with distinct metabolic profile and female gender bias in KDM6A mutation frequency. Cancer Cell 2017;32:701–715.e7.
[13] Marzouka N, Eriksson P, Rovira C, Liedberg F, Sjödahl G, Höglund M. A validation and extended description of the Lund taxonomy for urothelial carcinoma using the TCGA cohort. Sci Rep 2018;8:3737.
[14] Mo Q, Nikolos F, Chen F, et al. Prognostic power of a tumor differentiation gene signature for bladder urothelial carcinomas. J Natl Cancer Inst 2018;110:448–59.
[15] Lindskrog SV, Prip F, Lamy P, Taber A, et al. An integrated multi-omics analysis identifies prognostic molecular subtypes of non-muscle-invasive bladder cancer. Nat Commun 2021;12:2301.
[16] Kamoun A, de Reyniès A, Allory Y, et al. A consensus molecular classification of muscle-invasive bladder cancer. Eur Urol 2020;77:420–33.
[17] Mani DR, Krug K, Zhang B, et al. Cancer proteogenomics: current impact and future prospects. Nat Rev Cancer 2022;22:298–313.
[18] Rodriguez H, Zenklusen JC, Staudt LM, Doroshow JH, Lowy DR. The next horizon in precision oncology: proteogenomics to inform cancer diagnosis and treatment. Cell 2021;184:1661–70.
[19] Zhang B, Wang J, Wang X, et al. Proteogenomic characterization of human colon and rectal cancer. Nature 2014;513:382–7.
[20] Mertins P, Mani DR, Ruggles KV, et al. Proteogenomics connects somatic mutations to signalling in breast cancer. Nature 2016;534:55–62.
[21] Zhang H, Liu T, Zhang Z, et al. Integrated proteogenomic characterization of human high-grade serous ovarian cancer. Cell 2016;166:755–65.
[22] Forget A, Martignetti L, Puget S, et al. Aberrant ERBB4-SRC signaling as a hallmark of group 4 medulloblastoma revealed by integrative phosphoproteomic profiling. Cancer Cell 2018;34:379–395.e7.
[23] Clark DJ, Dhanasekaran SM, et al. Integrated proteogenomic characterization of clear cell renal cell carcinoma. Cell 2019;179:964–983.e31.
[24] Johansson HJ, Socciarelli F, Vacanti NM, et al. Breast cancer quantitative proteome and proteogenomic landscape. Nat Commun 2019;10:1600.
[25] Stroggilos R, Mokou M, Latosinska A, et al. Proteome-based classification of nonmuscle invasive bladder cancer. Int J Cancer 2020;146:281–94.
[26] Xu N, Yao Z, Shang G, et al. Integrated proteogenomic characterization of urothelial carcinoma of the bladder. J Hematol Oncol 2022;15:76.
[27] Casey RG, Catto JWF, Cheng L, et al. Diagnosis and management of urothelial carcinoma in situ of the lower urinary tract: a systematic review. Eur Urol 2015;67:876–88.
[28] Biton A, Bernard-Pierrot I, Lou Y, et al. Independent component analysis uncovers the landscape of the bladder tumor transcriptome and reveals insights into luminal and basal subtypes. Cell Rep 2014;9:1235–45.
[29] Sanchez-Quiles V, Shi M-J, Dingli F, et al. Triple extraction method enables high quality mass spectrometry-based proteomics and phospho-proteomics for eventual multi-omics integration studies. Proteomics 2021;21:e2000303.
[30] Geiger T, Cox J, Ostasiewicz P, Wisniewski JR, Mann M. Super-SILAC mix for quantitative proteomics of human tumor tissue. Nat Methods 2010;7:383–5.
[31] Becht E, Giraldo NA, Lacroix L, et al. Estimating the population abundance of tissue-infiltrating immune and stromal cell populations using gene expression. Genome Biol 2016;17:218.
[32] Argelaguet R, Velten B, Arnol D, et al. Multi-omics factor analysis a framework for unsupervised integration of multi-omics data sets. Mol Syst Biol 2018;14:e8124.
[33] Steele LP, Georgopoulos NT, Southgate J, Selby PJ, Trejdosiewicz LK. Differential susceptibility to TRAIL of normal versus malignant human urothelial cells. Cell Death Differ 2006;13:1564–76.
[34] Szliszka E, Mazur B, Zydowicz G, Czuba ZP, Król W. TRAIL-induced apoptosis and expression of death receptor TRAIL-R1 and TRAIL-R2 in bladder cancer cells. Folia Histochem Cytobiol 2009;47:579–85.
[35] Sun B, Moibi JA, Mak A, Xiao Z, Roa W, Moore RB. Response of bladder carcinoma cells to TRAIL and antisense oligonucleotide, Bcl-2 or clusterin treatments. J Urol 2009;181:1361–71.

[36] Shi M-J, Meng X-Y, Fontugne J, Chen C-L, Radvanyi F, Bernard-Pierrot I. Identification of new driver and passenger mutations within APOBEC-induced hotspot mutations in bladder cancer. Genome Med 2020;12:85.
[37] Mahe M, Dufour F, Neyret-Kahn H, et al. An FGFR3/MYC positive feedback loop provides new opportunities for targeted therapies in bladder cancers. EMBO Mol Med 2018;10:e8163.
[38] Shi M-J, Fontugne J, Moreno-Vega A, et al. FGFR3 mutational activation can induce luminal-like papillary bladder tumor formation and favors a male sex bias. Eur Urol 2023;83:70–81.
[39] Griffith TS, Kucaba TA, O'Donnell MA, et al. Sensitization of human bladder tumor cells to TNF-related apoptosis-inducing ligand (TRAIL)-induced apoptosis with a small molecule IAP antagonist. Apoptosis 2010;16:13–26.
[40] Amaravadi RK, Schilder RJ, Martin LP, et al. A phase I study of the SMAC-mimetic birinapant in adults with refractory solid tumors or lymphoma. Mol Cancer Ther 2015;14:2569–75.
[41] Sikic BI, Eckhardt SG, Gallant G, et al. Safety, pharmacokinetics (PK), and pharmacodynamics (PD) of HGS1029, an inhibitor of apoptosis protein (IAP) inhibitor, in patients (Pts) with advanced solid tumors: results of a phase I study. J Clin Oncol 2011;29:3008.
[42] Lincz L, Yeh T-X, Spencer A. TRAIL-induced eradication of primary tumour cells from multiple myeloma patient bone marrows is not related to TRAIL receptor expression or prior chemotherapy. Leukemia 2001;15(10):1650–7.

Please cite this article as: C.S. Groeneveld, V. Sanchez-Quiles, F. Dufour et al., Proteogenomic Characterization of Bladder Cancer Reveals Sensitivity to Apoptosis Induced by Tumor Necrosis Factor–related Apoptosis-inducing Ligand in *FGFR3*-mutated Tumors, Eur Urol (2023), https://doi.org/10.1016/j.eururo.2023.05.037